A MODEL TO STUDY THE REDUCTION OF TURBINE BLADE VIBRATION USING THE SNUBBING MECHANISM

Paolo Pennacchi, Steven Chatterton, Nicolò Bachschmid
Department of Mechanical Engineering
Politecnico di Milano
Via La Masa, 34, I–20156, Milan, Italy
paolo.pennacchi@polimi.it, nicolo.bachschmid@polimi.it, steven.chatterton@polimi.it

Emanuel Pesatori, Giorgio Turozzi
R&D Department
Franco Tosi Meccanica S.p.A.
P.zza Monumento 12, I–20025, Legnano (MI), Italy
emanuel.pesatori@francotosimeccanica.it, giorgio.turozzi@francotosimeccanica.it

ABSTRACT

Blade vibration reduction is an important task in high performance turbo machinery for power generation, in order to avoid the risk of blade failure due to the overcoming of fatigue limit. A possible way to obtain this result is a contact related phenomenon, i.e. by physically limiting the vibration amplitude on the blade tip leaving a small gap between the shrouds of adjacent blades. When the relative displacement between adjacent blades exceeds the gap, in a certain vibration mode of the blade row, a contact occurs between the shrouds, the relative motion is restricted and energy is dissipated by friction and impact during the contact. This is called the snubbing mechanism.

In this paper, an original simplified model of bladed disks, in which the snubbing mechanism can occur, is presented and numerical integration in time domain furnishes the time histories of the vibrations of the blades. The level of vibration reduction is then evaluated in some different modes that could be excited for instance by the fluid flow. It is also shown that unlucky combinations of system and excitation parameters can effect also a certain magnification instead of a reduction of the vibration amplitudes.

Experimental results on single blades and blade groups of a steam turbine are used to tune the parameters of the system.

1. INTRODUCTION

In the last decades machine manufacturers took great care about blade vibration reduction in high performance turbo machinery, to avoid fatigue crack development and consequent blade failures [1][2][3]. Blade vibrations are generally excited by the fluid flow and may become dangerous in case of resonance. Resonant conditions cannot always be avoided; therefore devices are needed to reduce the vibration amplitudes in these conditions. Energy dissipation, due to micro slipping friction in blade roots, by means of underplatform dampers [4][5][6][7][8][9] or friction rings [10][11][12], or in blade connecting wires, is useful to introduce damping in the system. Another way to obtain blade vibration reduction is limiting the vibration amplitude at the blade tip by leaving only a small gap between the shrouds of adjacent blades. In the vibration modes of the blade row in which the relative displacement between adjacent blades exceeds the gap, a contact occurs between the blade tips [13]. During the contact some energy is dissipated because the shock is not purely elastic and because there is friction between the contacting surfaces.

The relative vibration amplitude between adjacent blades is restricted and therefore also the absolute vibration amplitude is reduced with respect to the vibration amplitude for free standing blades (without contact). In the paper, this mechanism, called *snubbing*, is analyzed in dynamic conditions, taking into account impacts and rebounds and energy dissipation in different conditions.

Since it is not possible, for practical reasons, to measure snubbing effectiveness on a full scale real machine with working fluid, then an original simplified model of blade rows, in which the

blades are represented by their modal model, is introduced by the authors; integration in time domain is then performed and the time histories of the vibrations of the blades are displayed and analyzed. The bladed disk (composed of 120 blades) of a real machine is considered for the numerical analysis. The level of vibration reduction, in different modes that could be excited by the fluid flow, is then evaluated. It is also shown that unlucky combinations of system and excitation parameters can effect a certain magnification instead of a reduction of the vibration amplitudes in presence of contact on the shrouds.

In order to tune the parameters of the system and to give to the proposed model reliable inputs, experimental tests on single blade and groups of blades of a steam turbine for power generation have been performed and are briefly presented here.

The analysis of the effect of scatter friction on general contact surfaces or on bladed disks has attracted many researchers who have proposed different models for the friction interface elements (on both blade tips and roots) and different methods to calculate the response of bladed disks, modeled by accurate meshes of finite elements and associated friction interface elements. Anyhow they normally deal with turbine engines. Sanliturk and Ewins [14] analyzed the elliptical motion across a 2D friction contact interface and they modeled the response to steady state harmonic excitation by using an approximate first order harmonic balance method. Yang et al. in [15] simulated the harmonic response of a 3D friction contact surface by considering the stick-slip phenomenon, adding the nonlinear behavior of the equations in case of surface separation. In [16], Petrov and Ewins considered the 3D model of friction contact applied to the case of two turbine engine blades with friction contact at blade shrouds. Simple numerical time-domain integrations show a reduction of vibrations for harmonic forces applied at blade tips. Petrov in [17] developed a method for analyzing the nonlinear forced response of bladed disks as a function of the friction contact parameters, whereas the same author in [18], Götting et al. in [19] and Sextro et al. in [20] included the mistuning of the blade dynamic characteristics. Harish et al. in [21] and in [22] and Golden and Calcaterra in [23], investigated and modeled the friction contact between the blade root and the disk of a turbine engine for fretting fatigue analysis.

One very effective approach is described by Petrov and Ewins [24]. This last method allows reducing significantly the computation efforts, but is still too cumbersome to give an overview of the possible dynamic behaviors of such complex systems.

2. KINEMATICS OF BLADED DISK VIBRATION

The bladed disk considered in this paper are composed of 120 side entry 7.5” – 190.5 mm blades with firtree root and shroud on the blade tip (see figure 1).

Blades are assembled on the disk with a nominal gap g between the shrouds of two adjacent blades.

Since the nominal gap will not be exactly implemented, because of geometric tolerances, of positioning, of rotation and of untwisting of the blades, also the effects of bigger or smaller gaps than the nominal one, randomly distributed, are possible. The nominal gap is equal to 20μm for the bladed disk considered hereafter.

The vibration amplitude of the blades, along circumferential direction in their first modes, is limited by both the energy dissipation, caused by micro slipping friction, between the slot and the root, and by the contact with the adjacent blade, which generally does not vibrate with the same amplitude and phase. If, during the vibration, the relative displacement between two adjacent blades exceeds the gap, an impact and energy dissipation occurs causing the limitation of the vibration amplitude.

Figure 1: Bladed disk considered in the paper.

The different vibration modes of a bladed row, neglecting mistuning effects of the blades, are characterized by the presence of nodal diameters and consequent nodal points, in correspondence to which the mode amplitude is null. The mode with 0 nodal diameters is also called *umbrella mode* and all the blades move in phase with the same amplitude. Therefore the relative displacement between the adjacent blades is null. In the umbrella mode there is no amplitude limitation due to snubbing. The mode with 1 nodal diameter ($n=1$) has a sinusoidal distribution of the amplitudes around the row circumference, with half of the row that moves in phase opposition to the other. Thus, in this mode, a small relative displacement exists between the adjacent blades that have absolute displacements with small differences, being at different points of the sinusoid (see figure 2).

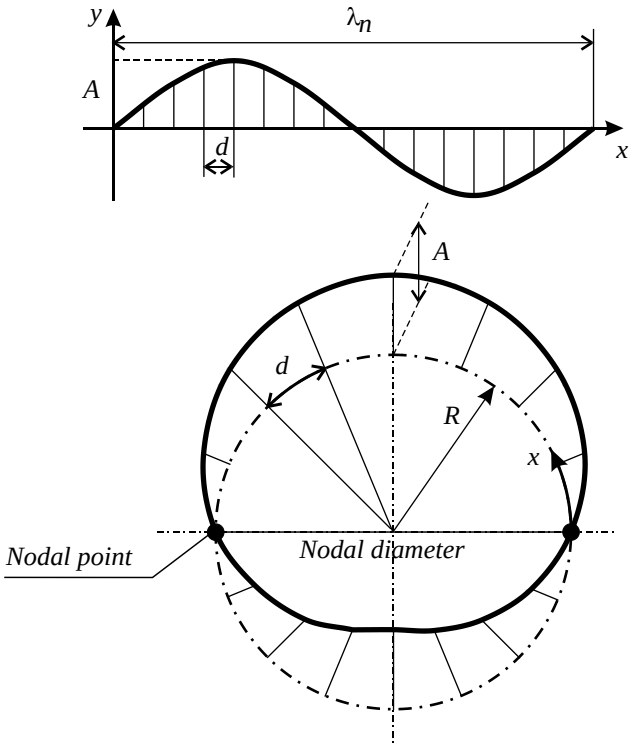

Figure 2: Distribution of the vibration amplitudes in the first mode ($n=1$) of a bladed disk.

3. FLUID FLOW EXCITATION

With regard to the excitation, which is mainly caused by the gas/steam flow constrained by the stator blade rows or by the nozzles for the machine types considered in this paper, the forcing system is non-moving in space. If the stator forces have a uniform distribution around the external

diameter, they cause a forced motion with 0 nodal diameters. On the contrary, if they have a non-uniform distribution, with different amplitudes in different angular positions, but periodic over a revolution, this periodic distribution in the space can be expanded in Fourier's series:

$$F(\theta) = F_0 + \sum_n F_n \sin\left(n\theta + \varphi_n\right) \tag{1}$$

where θ is the generic angular position of the stator force distribution and φ_n is the n-th phase.

In the relative motion of the rotating row, the angular force distribution in a fixed place is covered with the angular speed of the rotor, equal to Ω. Therefore, the angle θ covered by the first blade in time t is equal to Ωt and the force acting on the first blade is:

$$F_{(1)}(t) = F_0 + \sum_n F_n \sin\left(n\Omega t + \varphi_n\right) \tag{2}$$

Assuming for instance only the predominant n-th harmonic component of the force distribution, $F_0 = 0$ and $\varphi_n = 0$, the travelling wave force $F_{(k)}(t)$ acting on the k-th rotating blade is:

$$F_{(k)}(t) = F_n \sin\left(n\Omega t + n\frac{2\pi}{z}(k-1)\right) \qquad k = 1,\ldots,z \tag{3}$$

If the frequency corresponding to the rotating speed Ω is f_0 and the exciting frequency is nf_0, then the blades of the row vibrate with the frequency nf_0 and with the mode having n nodal diameters. Therefore n is called *engine order* from the point of view of the excitation in the time domain and *number of nodal diameters* from the point of view of the response in the space domain. If the excitation frequency nf_0 is equal to the natural frequency associated to the mode with n nodal diameters, then we have resonance and the blade vibration amplitudes become rather high. Otherwise, the deflection shape is the same but the amplitudes remain small.

Furthermore, if F_0 and F_n are not constant, but have variable components due for instance to flow turbulence, and have the form of:

$$\begin{aligned} F_0 &= F_{0_m} + \Delta F_0 \sin 2\pi f_t t = F_{0_m} + \Delta F_0 \sin \omega_t t \\ F_n &= F_{n_m} + \Delta F_n \sin 2\pi f_t t = F_{n_m} + \Delta F_n \sin \omega_t t \end{aligned} \tag{4}$$

where ω_t is the turbulence circular frequency and the excitations acting on the rotating row are:

$$F_{(k)}(t) = F_{0_m} + \Delta F_0 \sin \omega_t t + \sum_n \left(F_{n_m} + \Delta F_n \sin \omega_t t\right) \sin\left(n\Omega t + n\frac{2\pi}{z}(k-1) + \varphi_n\right) \tag{5}$$

Apart from the constant force F_{0_m} due to the fluid, there are 3 different types of excitation:

$$\begin{aligned} F_{(k)}^{(1)}(t) &= \Delta F_0 \sin \omega_t t \\ F_{(k)}^{(2)}(t) &= \sum_n F_{n_m} \sin\left(n\Omega t + n\frac{2\pi}{z}(k-1) + \varphi_n\right) \\ F_{(k)}^{(3)}(t) &= \sum_n \Delta F_n \sin\left(n\Omega t + n\frac{2\pi}{z}(k-1) + \varphi_n\right) \sin \omega_t t \end{aligned} \tag{6}$$

- force $F_{(k)}^{(1)}(t)$ excites the umbrella mode;
- force $F_{(k)}^{(2)}(t)$ excites the modes with n nodal diameters, as previously described;
- force $F_{(k)}^{(3)}(t)$ causes the excitations:

$$F_{(k)}^{(3)}(t) = \frac{1}{2}\sum_n \Delta F_n \left(\cos\left(\left(\omega_t - n\Omega\right)t - \left(n\frac{2\pi}{z}(k-1) + \varphi_n\right)\right) - \cos\left(\left(\omega_t + n\Omega\right)t + \left(n\frac{2\pi}{z}(k-1) + \varphi_n\right)\right)\right) \tag{7}$$

These last forces can excite natural modes of the row only if $\omega_t \pm n\Omega$ corresponds to the circular natural frequency of the n-th mode.

Moreover, natural modes of the row have frequencies that are less than the natural frequency of the single blade alone due to the additional stiffness introduced by the disk, strongly dependent on the nodal diameter. These frequencies tend to a constant value (i.e. to the natural frequency of the single blade) as n becomes close to z [24]. In the following a simple model is introduced to analyze some dynamic effects of the snubbing mechanism.

4. A SIMPLE MODEL FOR THE SNUBBING MECHANISM

On the basis of the previous considerations about fluid excitation and the possibility of impacts between the shrouds, dynamics effects could not be neglected, thus an original dynamic model for the snubbing is here proposed. Obviously, the model is simplified and cannot take into account the real blade models, but it is addressed to show basic characteristics of the snubbing mechanism and highlights some aspects that can be extended to a more sophisticated modelling. The simplified model does not require huge computational time and resources, which are on the contrary necessary if 3D nonlinear calculation is performed.

Let us consider figure 3 that shows a sketch of the considered bladed disk. The number of the blades is z, they are ordered and, due to the radial symmetry of the system, blade 1 follows blade z and precedes blade 2. Each blade j is connected to its root r_j and both have a degree of freedom represented respectively by the generalized displacements x_j and y_j. Lumped masses m_j and m_{r_j} are attributed to each blade and root respectively. Coefficients k_j and c_j represent the blade modal stiffness and damping, while the inter-root stiffness and damping are represented by coefficients $k_{r_{j(j+1)}}$ and $c_{r_{j(j+1)}}$ The model of the continuity of the roots on the disk and other effects, like friction, in the connection between the root and the blade, is represented by these coefficients.

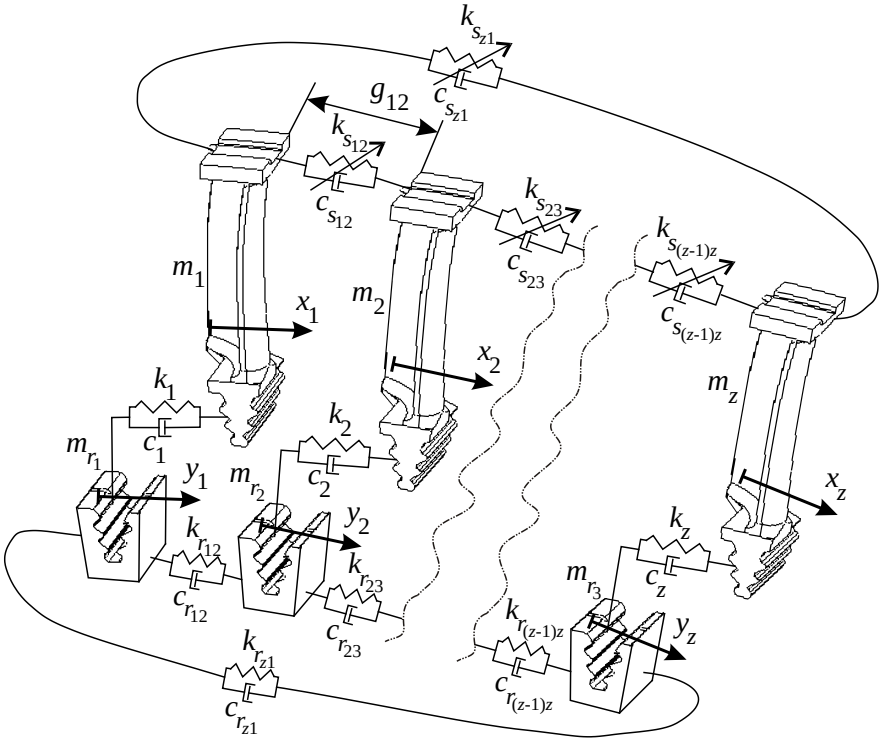

Figure 3: Model of the bladed row.

These assumptions correspond to:

i) use a modal approach for the blade, that is acceptable because the snubbing effect modeled here occurs when the blades are excited in resonance; m_j is the modal mass of the blades, k_j its modal stiffness and c_j its modal damping;

ii) consider the roots as very, but not infinitely, rigid because stiffnesses $k_{r_{j(j+1)}}$ are much greater than k_j.

Finally the inter-shroud stiffness $k_{s_{j(j+1)}}$ and damping $c_{s_{j(j+1)}}$ are different from zero only when two subsequent shrouds of blade j and $j+1$ are in contact. This condition is verified when:

$$x_j - x_{j+1} > g_{j(j+1)} \tag{8}$$

i.e. when the difference between the displacements of blades j and $j+1$ is greater than the nominal assembling gap $g_{j(j+1)}$ between them.

Lagrange's equation approach is used to define the analytical model of the system. The first step is to define the set of values for the index i used for inter-root and inter-shroud coefficients. This index, which can conveniently be used to formalize the equations, belongs to the set I defined as:

$$I = \{1, 2, \ldots, z, 1\} \tag{9}$$

so that the cardinality of I is $z+1$. This reflects the cyclicity of the considered system.

Kinetic energy of the system is equal to:

$$T = \frac{1}{2}\sum_{j=1}^{z} m_j \dot{x}_j^2 + \frac{1}{2}\sum_{j=1}^{z} m_{r_j} \dot{y}_j^2 \tag{10}$$

Linear elastic potential energy is:

$$V = \frac{1}{2}\sum_{j=1}^{z} k_j \left(x_j - y_j\right)^2 + \frac{1}{2}\sum_{j=1}^{z} k_{r_{I_j I_{j+1}}} \left(y_{I_j} - y_{I_{j+1}}\right)^2 \tag{11}$$

Similarly, the linear damping function is:

$$R = \frac{1}{2}\sum_{j=1}^{z} c_j \left(\dot{x}_j - \dot{y}_j\right)^2 + \frac{1}{2}\sum_{j=1}^{z} c_{r_{I_j I_{j+1}}} \left(\dot{y}_{I_j} - \dot{y}_{I_{j+1}}\right)^2 \tag{12}$$

Apart from external forcing F_j acting on each blade, a nonlinear inter-shroud force is defined as:

$$F_{s_{I_j I_{j+1}}} = \eta_{I_j I_{j+1}} \left(-k_{s_{I_j I_{j+1}}} \left(x_{I_j} - x_{I_{j+1}} - g_{I_j I_{j+1}}\right) - c_{s_{I_j I_{j+1}}} \left(\dot{x}_{I_j} - \dot{x}_{I_{j+1}}\right)\right), \; j \in [1, z] \tag{13}$$

where $\eta_{I_j I_{j+1}}$ is a Boolean variable, used to take into consideration if the contact between the shrouds exists, and is defined as:

$$\eta_{I_j I_{j+1}} = \begin{cases} 1, & x_{I_j} - x_{I_{j+1}} > g_{I_j I_{j+1}} \\ 0, & x_{I_j} - x_{I_{j+1}} \le g_{I_j I_{j+1}} \end{cases}, \; j \in [1, z] \quad \begin{matrix} \text{contact} \\ \text{no contact} \end{matrix} \tag{14}$$

The virtual work of the forces is:

$$\delta U = \sum_{j=1}^{z} F_j \, \delta x_j + \sum_{j=1}^{z} F_{s_{I_j I_{j+1}}} \, \delta\left(x_{I_j} - x_{I_{j+1}} - g_{I_j I_{j+1}}\right) \tag{15}$$

Then, the degrees of freedom are grouped in vector $\mathbf{q}$ as follows:

$$\mathbf{q} = \begin{Bmatrix} x_1 & y_1 & x_2 & y_2 & \cdots & x_z & y_z \end{Bmatrix}^{\mathrm{T}} \tag{16}$$

and the system of equations can be written in the canonical form as:

$$[\mathbf{M}]\ddot{\mathbf{q}} + \left([\mathbf{C}] + [\mathbf{C}_r] + [\mathbf{C}_s(\mathbf{q})]\right)\dot{\mathbf{q}} + \left([\mathbf{K}] + [\mathbf{K}_r] + [\mathbf{K}_s(\mathbf{q})]\right)\mathbf{q} = \mathbf{F}_s^{(s)}(\mathbf{q}) + \mathbf{F} \tag{17}$$

where matrices on the left hand side of eq. (17) are defined as:

- the generalized mass matrix:

$$[\mathbf{M}]=\begin{bmatrix} m_1 & 0 & 0 & 0 & \cdots & 0 & 0 \\ 0 & m_{r_1} & 0 & 0 & \cdots & 0 & 0 \\ 0 & 0 & m_2 & 0 & \cdots & 0 & 0 \\ 0 & 0 & 0 & m_{r_2} & \cdots & 0 & 0 \\ \vdots & \vdots & \vdots & \vdots & \ddots & \vdots & \vdots \\ 0 & 0 & 0 & 0 & \cdots & m_z & 0 \\ 0 & 0 & 0 & 0 & \cdots & 0 & m_{r_z} \end{bmatrix} \tag{18}$$

- the blade-root damping matrix:

$$[\mathbf{C}]=\begin{bmatrix} c_1 & -c_1 & 0 & 0 & \cdots & 0 & 0 \\ -c_1 & c_1 & 0 & 0 & \cdots & 0 & 0 \\ 0 & 0 & c_2 & -c_2 & \cdots & 0 & 0 \\ 0 & 0 & -c_2 & c_2 & \cdots & 0 & 0 \\ \vdots & \vdots & \vdots & \vdots & \ddots & \vdots & \vdots \\ 0 & 0 & 0 & 0 & \cdots & c_z & -c_z \\ 0 & 0 & 0 & 0 & \cdots & -c_z & c_z \end{bmatrix} \tag{19}$$

- the inter-root damping matrix:

$$[\mathbf{C}_r]=\begin{bmatrix} 0 & 0 & 0 & 0 & \cdots & 0 & 0 \\ 0 & c_{r_{z1}}+c_{r_{12}} & 0 & -c_{r_{12}} & \cdots & 0 & -c_{r_{z1}} \\ 0 & 0 & 0 & 0 & \cdots & 0 & 0 \\ 0 & -c_{r_{12}} & 0 & c_{r_{12}}+c_{r_{23}} & \cdots & 0 & 0 \\ \vdots & \vdots & \vdots & \vdots & \ddots & \vdots & \vdots \\ 0 & 0 & 0 & 0 & \cdots & 0 & 0 \\ 0 & -c_{r_{z1}} & 0 & 0 & \cdots & 0 & c_{r_{(z-1)z}}+c_{r_{z1}} \end{bmatrix} \tag{20}$$

- the inter-shroud damping matrix, the general element of which is different from zero only when two subsequent shrouds of blade j and $j+1$ are in contact:

$$[\mathbf{C}_s(\mathbf{q})]=\begin{bmatrix} \eta_{z1}c_{s_{z1}}+\eta_{12}c_{s_{12}} & 0 & -\eta_{12}c_{s_{12}} & 0 & \cdots & -\eta_{z1}c_{s_{z1}} & 0 \\ 0 & 0 & 0 & 0 & \cdots & 0 & 0 \\ -\eta_{12}c_{s_{12}} & 0 & \eta_{12}c_{s_{12}}+\eta_{23}c_{s_{23}} & 0 & \cdots & 0 & 0 \\ 0 & 0 & 0 & 0 & \cdots & 0 & 0 \\ \vdots & \vdots & \vdots & \vdots & \ddots & \vdots & \vdots \\ -\eta_{z1}c_{s_{z1}} & 0 & 0 & 0 & \cdots & \eta_{(z-1)z}c_{s_{(z-1)z}}+\eta_{z1}c_{s_{z1}} & 0 \\ 0 & 0 & 0 & 0 & \cdots & 0 & 0 \end{bmatrix} \tag{21}$$

- the blade-root stiffness matrix $[\mathbf{K}]$, the inter-root stiffness matrix $[\mathbf{K}_r]$ and the the inter-shroud stiffness matrix $[\mathbf{K}_s(\mathbf{q})]$ have the same structure of the corresponding damping matrices.

The forcing system on the right hand side of eq. (17) consists of:

- the inter-shroud static stiffness force, the general element of which is different from zero only when two subsequent shrouds of blade j and $j+1$ are in contact:

$$\mathbf{F}_s^{(s)} = \begin{Bmatrix} \left(\eta_{z1} k_{s_{z1}} g_{z1} + \eta_{12} k_{s_{12}} g_{12}\right) & 0 & \left(\eta_{12} k_{s_{12}} g_{12} + \eta_{23} k_{s_{23}} g_{23}\right) & 0 & \cdots \\ \cdots & \left(\eta_{(z-1)z} k_{s_{(z-1)z}} g_{(z-1)z} + \eta_{z1} k_{s_{z1}} g_{z1}\right) & 0 & & \end{Bmatrix}^{\mathrm{T}} \tag{22}$$

- the external forces acting on the blades:

$$\mathbf{F} = \begin{Bmatrix} F_{(1)} & 0 & F_{(2)} & 0 & \cdots & F_{(z)} & 0 \end{Bmatrix}^{\mathrm{T}} \tag{23}$$

Due to the presence of the terms $[\mathbf{C}_s(\mathbf{q})]$, $[\mathbf{K}_s(\mathbf{q})]$ and $\mathbf{F}_s^{(s)}(\mathbf{q})$ that depend on occurrence of the contacts on the shrouds, eq. (17) represents a nonlinear system. Its integration in the time domain is performed by means of Newmark's implicit method, in which the values of $\eta_{i(i+1)}$ are determined at each time step by means of eq. (14). The algorithm is the following:

1. Starting from a suitable set of initial conditions $\mathbf{q}_0$ and $\dot{\mathbf{q}}_0$ for $t = 0$, the force vectors $\mathbf{F}_s^{(s)}(\mathbf{q}_0)$ and $\mathbf{F}(0)$ are calculated.
2. The initial acceleration vector is calculated by:

$$\ddot{\mathbf{q}}_0 = [\mathbf{M}]^{-1}\left(\mathbf{F}_s^{(s)}(\mathbf{q}_0) + \mathbf{F}(0) - \left([\mathbf{C}] + [\mathbf{C}_r] + [\mathbf{C}_s(\mathbf{q}_0)]\right)\dot{\mathbf{q}}_0 - \left([\mathbf{K}] + [\mathbf{K}_r] + [\mathbf{K}_s(\mathbf{q}_0)]\right)\mathbf{q}_0\right) \tag{24}$$

3. Starting from the first time step, in a general time step k-th, the new force vectors $\mathbf{F}_s^{(s)}(\mathbf{q}_{t=t_{k-1}})$ and $\mathbf{F}(t_k)$ are calculated and the generalized displacements, accelerations and velocities are equal to:

$$\begin{aligned} \mathbf{q}_k = & \left[\frac{1}{a\,\Delta t^2}[\mathbf{M}] + \frac{b}{a\,\Delta t}\left([\mathbf{C}] + [\mathbf{C}_r] + [\mathbf{C}_s(\mathbf{q}_{k-1})]\right) + \left([\mathbf{K}] + [\mathbf{K}_r] + [\mathbf{K}_s(\mathbf{q}_{k-1})]\right)\right]^{-1} \cdot \\ & \cdot \left(\begin{array}{l} \mathbf{F}_s^{(s)}(\mathbf{q}_{k-1}) + \mathbf{F}(t_{k-1}) + \left[\frac{1}{a\,\Delta t^2}[\mathbf{M}] + \frac{b}{a\,\Delta t}\left([\mathbf{C}] + [\mathbf{C}_r] + [\mathbf{C}_s(\mathbf{q}_{k-1})]\right)\right]\mathbf{q}_{k-1} + \\ + \left[\frac{1}{a\,\Delta t}[\mathbf{M}] - \left(1 - \frac{b}{a}\right)\left([\mathbf{C}] + [\mathbf{C}_r] + [\mathbf{C}_s(\mathbf{q}_{k-1})]\right)\right]\dot{\mathbf{q}}_{k-1} + \left[\begin{array}{l} \frac{1}{a}\left(\frac{1}{2} - a\right)[\mathbf{M}] - \Delta t\left(1 - \frac{b}{2a}\right)\cdot \\ \cdot\left([\mathbf{C}] + [\mathbf{C}_r] + [\mathbf{C}_s(\mathbf{q}_{k-1})]\right) \end{array}\right]\ddot{\mathbf{q}}_{k-1} \end{array} \right) \end{aligned} \tag{25}$$

$$\ddot{\mathbf{q}}_k = \frac{1}{a\,\Delta t^2}\left(\mathbf{q}_k - \mathbf{q}_{k-1} - \dot{\mathbf{q}}_{k-1}\Delta t\right) - \frac{1}{a}\left(\frac{1}{2} - a\right)\ddot{\mathbf{q}}_{k-1} \tag{26}$$

$$\dot{\mathbf{q}}_k = \frac{b}{a\,\Delta t}\left(\mathbf{q}_k - \mathbf{q}_{k-1}\right) + \left(1 - \frac{b}{a}\right)\dot{\mathbf{q}}_{k-1} + \Delta t\left(1 - \frac{b}{2a}\right)\ddot{\mathbf{q}}_{k-1} \tag{27}$$

The constants a and b of Newmark's method are assumed respectively equal to 0.25 and 0.5; this is equivalent to the "trapezium rule" and assures that the implicit integration is unconditionally stable, without adding numerical spurious damping (high values of b). In fact it can be proven that Newmark's method is unconditionally stable if $b \geq 0.5$ and $a \geq 0.25(0.5 + b)^2$.

5. IDENTIFICATION OF BLADE PARAMETERS

In order to identify the modal parameters of the considered blade, a suitable test-rig has been realized. The test-rig, called hereafter *test-block*, is composed of a sector of the disk with slots and blades (see figure 4). Obviously the test-block cannot reproduce the cyclicity of the entire bladed disk and it is employed only for model parameter tuning.

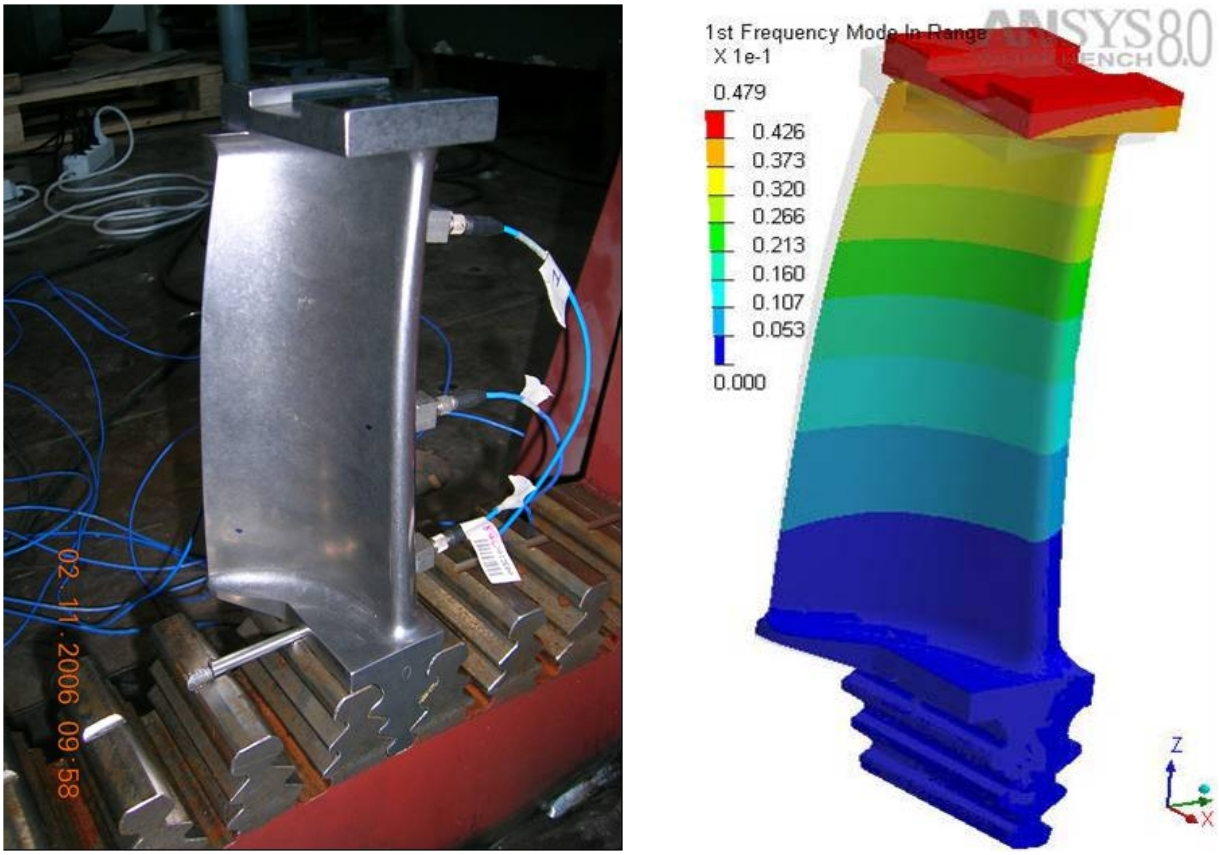

Figure 4: Single blade connection to the test-block, layout of accelerometer for impact tests and first mode shape calculated by means of a FEM software.

In the actual turbine, the blade root is hold in place in the slot simply by means of a pin. The centrifugal field during disk rotation pulls the blade in radial direction and causes the tightening of the firtree root in the slot, so that the constraint becomes rather rigid. This special effect has been reproduced in two different ways:

- for a single blade, a calibrated pin was used in order to force the contact between the firtree root and the slot (see figure 4);
- for the blade group, very stiff glue (araldite) was used between the firtree root and the slot and calibrated shims were inserted between the shrouds until glue hardening (see figure 7).

Centrifugal field has also the effect of general stiffening of the bladed disk of the real machine. This aspect cannot be reproduced by means of the test-block, but this is not relevant for the use of the model, since stiffness parameters can be also evaluated by means of finite element models, whilst it is possible to suppose that damping parameters are less sensible to the rotation, once correct constraints are reproduced.

Six piezo-electric accelerometers of negligible mass have been installed on the leading and trailing edges of the blade and impact tests allowed to identify natural frequencies and mode shapes of the blade. Finite element models showed excellent correspondence with experimental results. The first mode is considered in the study, since it is rather similar to a cantilever beam, in which the maximum displacement is in correspondence of the shroud. This is also confirmed by FEM analysis.

The first step was the evaluation of the blade root – slot damping and a single instrumented blade connected to the test-block has been used.

Even if impact tests allowed natural frequencies to be identified, it has been preferred to perform also forced response tests in order to accurately identify the blade modal parameters, especially with regard to the damping, the identification of which is rather critical, as reported also in [25].

To obtain the forced response, the shroud was connected to an electro-magnetic exciter by means of a negligible mass spring, which uncouples the blade from the exciter. The vibration in correspondence of the shroud is measured by means of a piezo-electric accelerometer (figure 5) of negligible mass compared to that of the system. The effect of the exciter and of the accelerometers on the dynamics of the system is negligible.

Figure 5: Excitation of the blade.

The frequency of the excitation is changed in a sweep at a rate of 0.1 Hz/s, in the neighborhood of the first natural frequency f_b, equal to 390.9 Hz. The experimental transfer function, between the shroud displacement and the excitation, is shown in figure 6 and allows the dimensionless damping to be evaluated[(1)].

[(1)] Note for the editor: actual damping value cannot be published for confidential reasons.

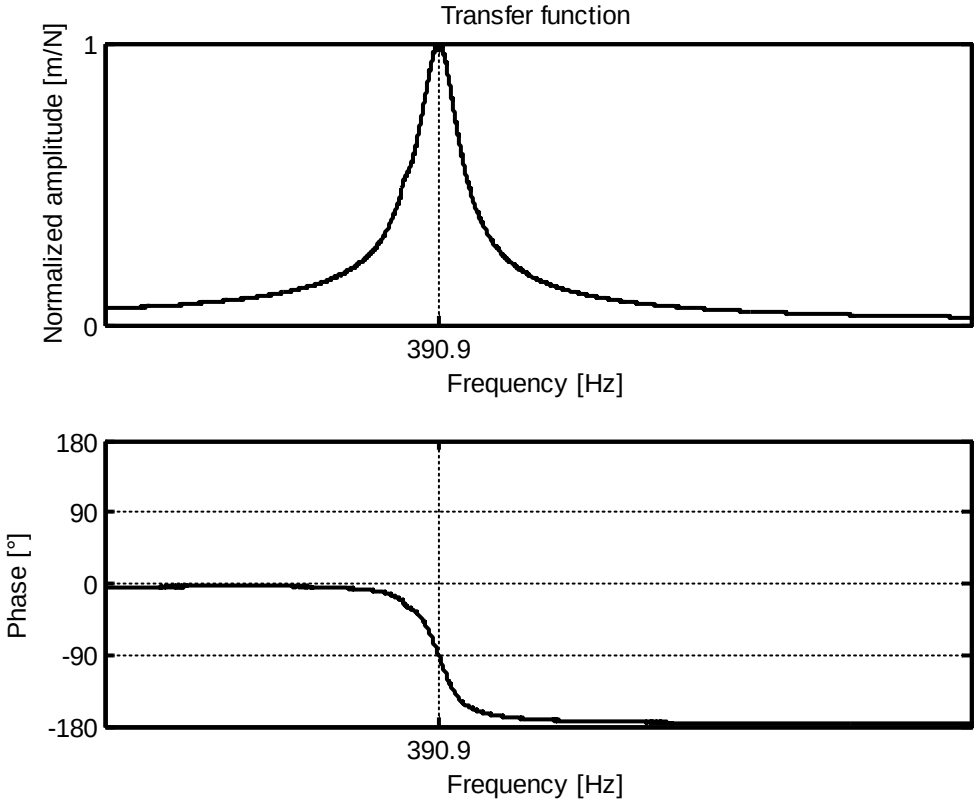

Figure 6: Transfer function for the single blade.

The second step was the determination of the equivalent damping during shroud contacts. In this case a group of blades was installed in the test-block (see figure 7) and accelerometers were installed on the lateral sides of the shrouds. Once again the central blade was excited in a frequency range, close to the first natural frequency. When the vibration amplitude exceeds the gap, shrouds come in contact and the measured response revealed to be as "cut" comparing to the response of the single blade. Figure 8 shows the vibration in case of no-contact and contact during a slow frequency sweep.

The comparison of the single free blade response and that of the same blade grouped, with the same type of excitation, allowed defining an equivalent damping generated by the snubbing effect, on the basis of the additional energy dissipated during the contact. This damping resulted to be much higher than the damping of the single blade[(2)].

6. SIMULATION OF SNUBBING EFFECT

The blade modal parameters have been set in the simplified numerical model described in section 4 in order to simulate the snubbing effect for the considered bladed disk at the first natural frequency of the blade. Modal blade mass m_j was considered unitary and modal stiffness k_j and dimensional damping c_j calculated accordingly. Inter-shroud damping $c_{s_{j(j+1)}}$ was obtained by means of the experimental tests described before, while the stiffness value of the bladed disk with continuous shrouding was used for inter-shroud stiffness $k_{s_{j(j+1)}}$.

Root mass m_{r_j} and stiffness k_{r_j} were obtained using the finite element model of the disk, while structural damping was used for the damping value c_{r_j}. Several numerical simulations are hereafter shown using the time step equal to 1e–5 s.

The gaps considered in the simulations have a random variation of 10%with respect to the nominal value of 20μm, uniformly distributed.

[(2)] Note for the editor: actual damping value cannot be published for confidential reasons.

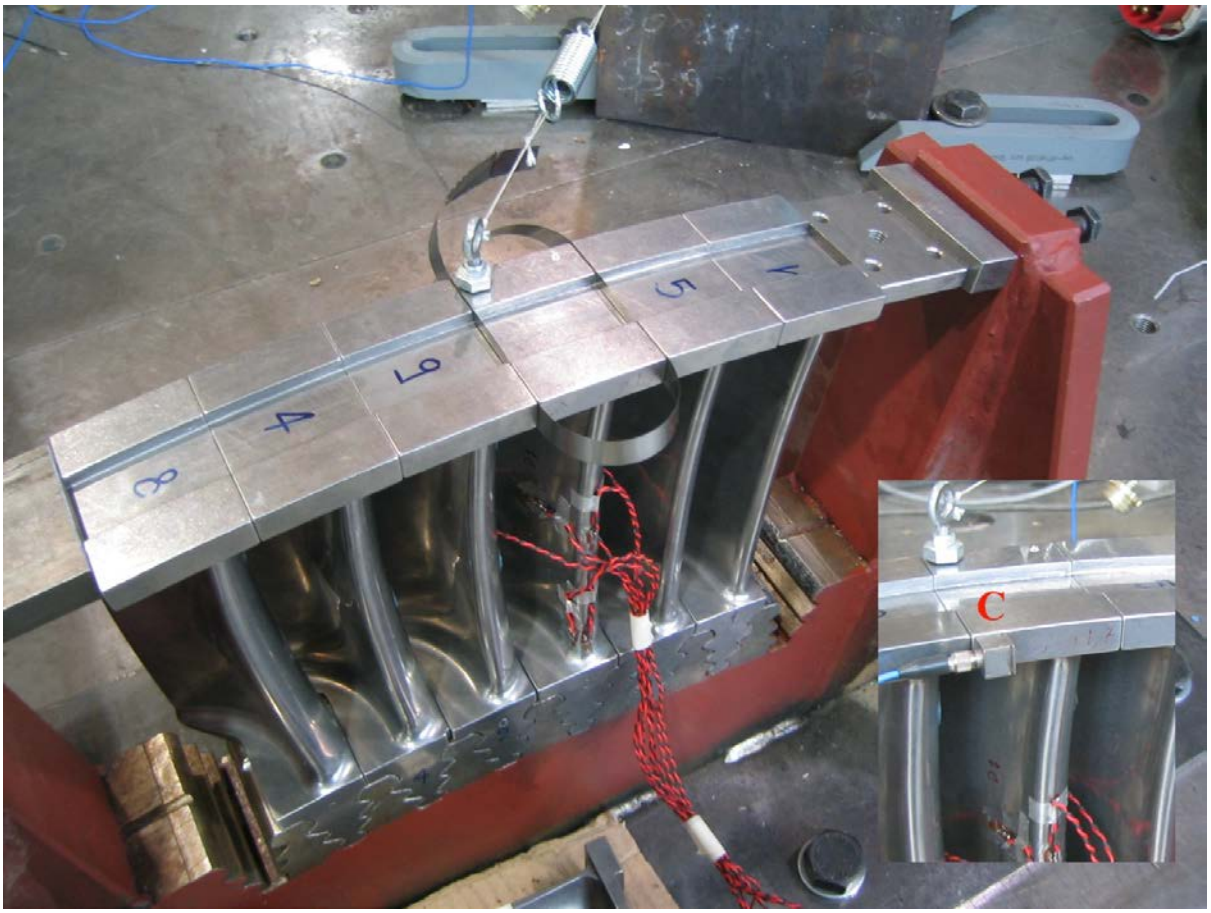

Figure 7: Test-block with a group of blade and installation of accelerometer on the shroud. Temporary shims to assure calibrated gap during glue hardening are visible.

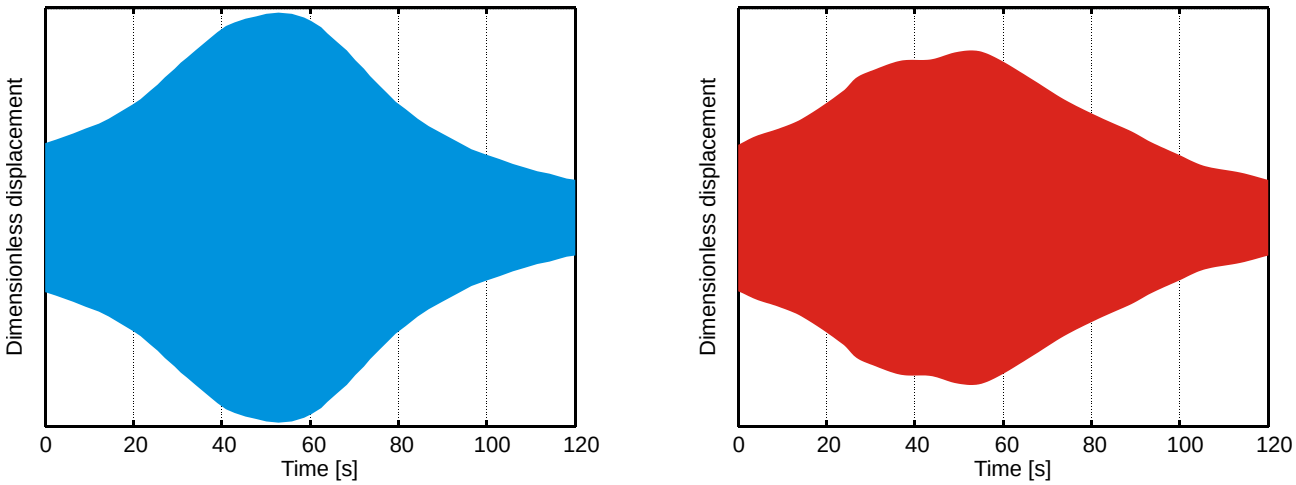

Figure 8: Vibration response during a frequency sweep. Comparing the left figure relative to a single blade to the right one where shroud contacts occur, the "cut" due to snubbing mechanism is evident.

With regards to the eigenfrequencies of the bladed disk obtained using the model and the modal blade parameters, figure 9 shows the system eigenfrequencies as a function of the nodal diameter number. Note that the eigenfrequencies tends asymptotically to the blade natural frequency. If the blades were always in contact, as in integral shroud condition, i.e. no gaps exist, the system becomes stiffer and a similar diagram to figure 9 is obtained but with a higher asymptotic value at about 1785 Hz.

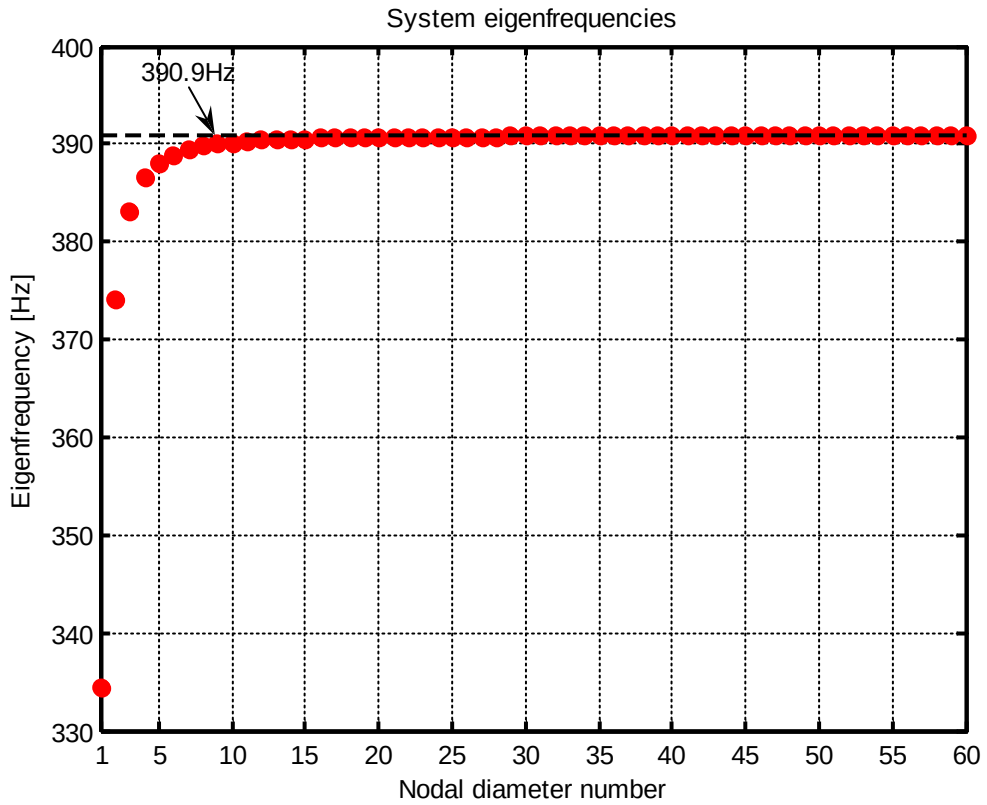

Figure 9: System eigenfrequencies as a function of the nodal diameter number.

6.1 Blade excitation by a travelling wave

In a rotating bladed disk a travelling wave is excited by the stationary force distribution. In this case the k-th element of the exciting forces vector of eq. (23) is given by eq. (3), where only the n-th harmonic component is considered. Figure 10 shows the results obtained starting from initial null conditions and considering the external excitation on the row having the amplitude of 150 N, the rotating frequency $f_0 = 50\,\text{Hz}$ and 8 nodal diameters. Thus the equivalent excitation frequency is 400 Hz, close to the eigenfrequency associated to 8 nodal diameters (see figure 9), and the system is close to the resonant condition.

The effectiveness of the snubbing mechanism is evident in this case, by comparing the time histories of the vibrations of the generalized displacements of a blade of the row, without (i.e. the blade is free to vibrate, no contact occurs and all $\eta_{i(i+1)}$ Boolean variables are equal to 0) and with the snubbing effect, which are displayed in the top of figure 10. The RMS value of the vibration amplitude is $x_{1,s}^{\text{RMS}} = 47.9\,\mu\text{m}$ in case of snubbing vs. $x_1^{\text{RMS}} = 335.0\,\mu\text{m}$ in case of free blades with a reduction of slightly less than an order of magnitude ($x_{1,s}^{\text{RMS}} / x_1^{\text{RMS}} = 0.143$).

The lower part of figure 10 shows the succession of the Boolean variables $\eta_{(i-1)i}$ and $\eta_{i(i+1)}$, which indicates whether the blade is in contact with an adjacent blade in case of snubbing. The close-up in figure 11, which considers the initial 0.05 s of the simulation, shows that the blades are not always in contact. It is easy to see that without the snubbing effect the vibration amplitude displays an increasing trend that is linear in its first stage, accordingly to the damped forced response of a linear system, and tends asymptotically to a steady value. In presence of the snubbing effect, the excitation frequency is no more immediately identifiable from the time response.

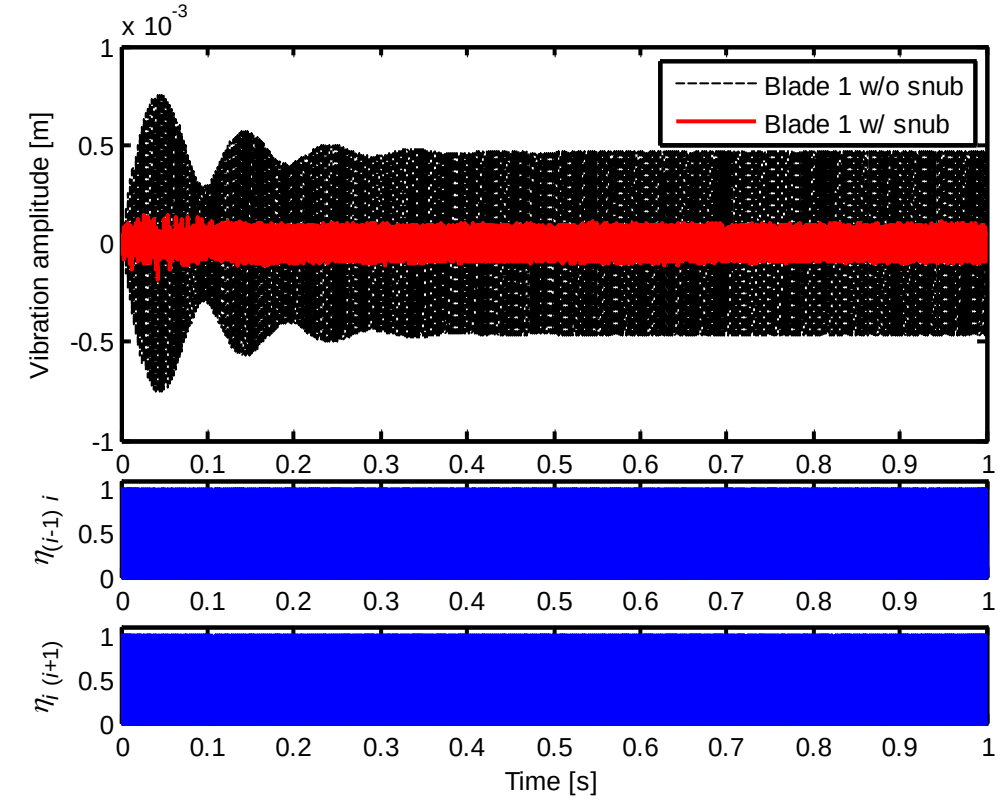

Figure 10: Time response of blade 1 with travelling wave, n = 8, F_8 = 150 N, f_0 = 50 Hz.

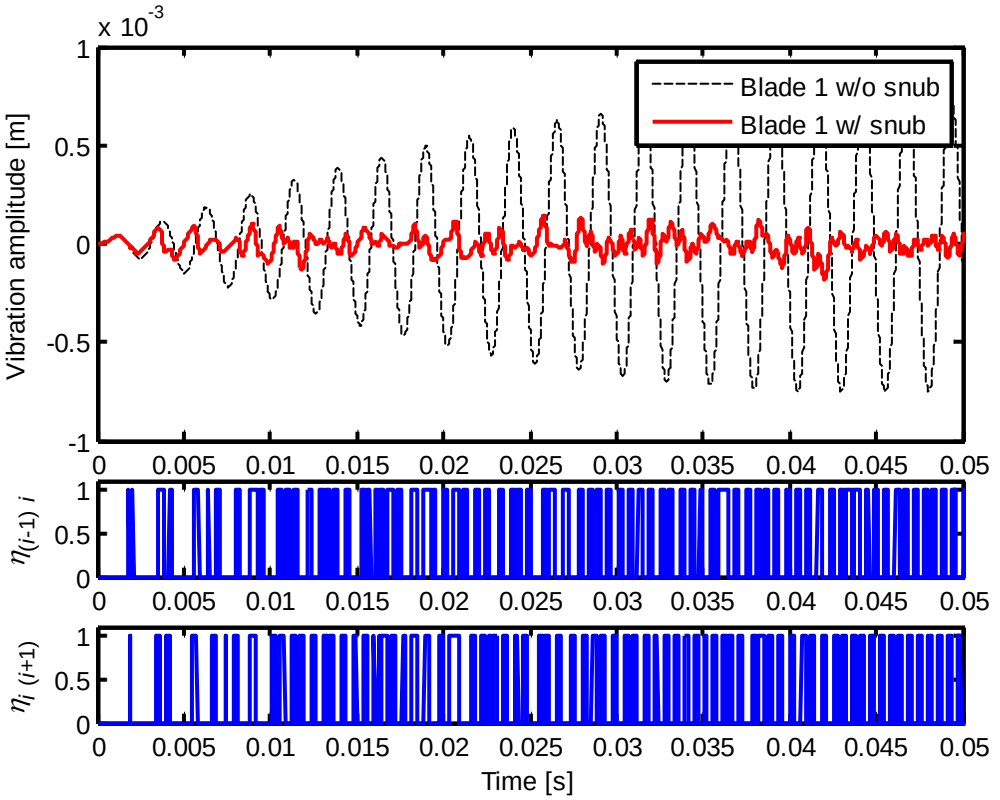

Figure 11: Close-up of figure 10.

The steady-state spectrum, considering the last 2^{15} samples of the simulation of the blade vibration with snubbing is shown in figure 12, which reveals that a kind of resonance is excited

when the shrouds get in contact, with relevant sidebands spaced of 400 Hz. The high frequency f_s of this vibration, about 1780 Hz, corresponds roughly to the eigenfrequency of the bladed disk with integral (i.e. continuous) shrouding. The presence of the high frequency component and its sidebands are ascribed to nonlinear effects due to the shroud intermittent contacts.

Similar results are obtained for the other blades of the row, not reported for brevity.

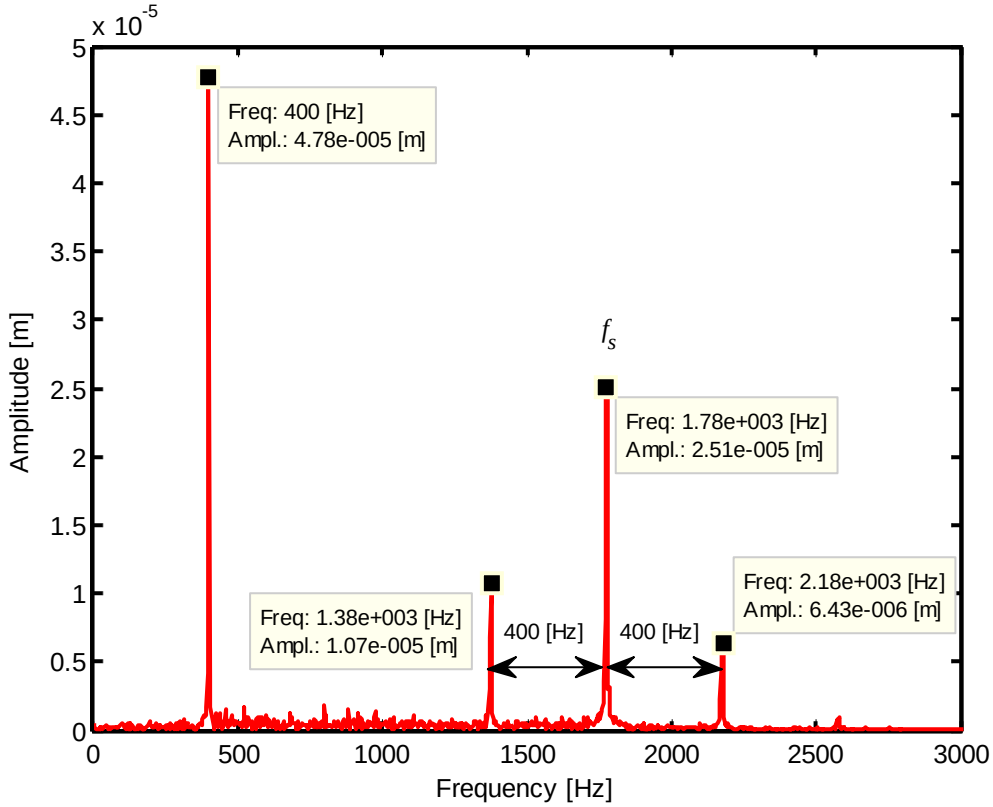

Figure 12: Vibration spectrum of blade 1 with snubbing and travelling wave, n = 8, F_8 = 150 N, f_0 = 50 .

6.2 Blade excitation by a travelling wave and turbulence

In a second set of simulations the turbulence is included, considering only the 3rd term of eq. (6) and the n-th harmonic component, i.e.:

$$F_{(k)}(t) = \Delta F_n \sin\left(n\Omega t + n\frac{2\pi}{z}(k-1)\right)\sin \omega_t t \tag{28}$$

Simulations are performed with different values of n: 4, 6 and 8. The system has been excited with a frequency close to the natural frequency of the single blade i.e. $f_b = 390.9\,\text{Hz}$, so that the corresponding values of the turbulence frequencies ω_t are given by:

$$\left|\omega_t \pm n\Omega\right| = 2\pi f_b \tag{29}$$

Figure 13-figure 15 show the time histories of the first blade for the three orders n considered. Since the excitation frequency is for all the cases close to the eigenfrequency of the mode and the system is close to the resonant condition, snubbing mechanism is effective for the vibration reduction with respect to the bladed disk, but without contacts on the shrouds, in the same exciting condition. These results are summarized in table 1. The lower part of the figures indicates that contact on the shrouds occurs and the close-ups indicate that they are intermittent.

Table 1: Comparison between RMS vibration amplitude in case of snubbing and free blades.

n	$x_{1,s}^{\mathrm{RMS}}$	x_1^{RMS}	$x_{1,s}^{\mathrm{RMS}} / x_1^{\mathrm{RMS}}$
4	72.6 µm	372.7 µm	0.195
6	42.4 µm	654.6 µm	0.065
8	40.0 µm	818.7 µm	0.049

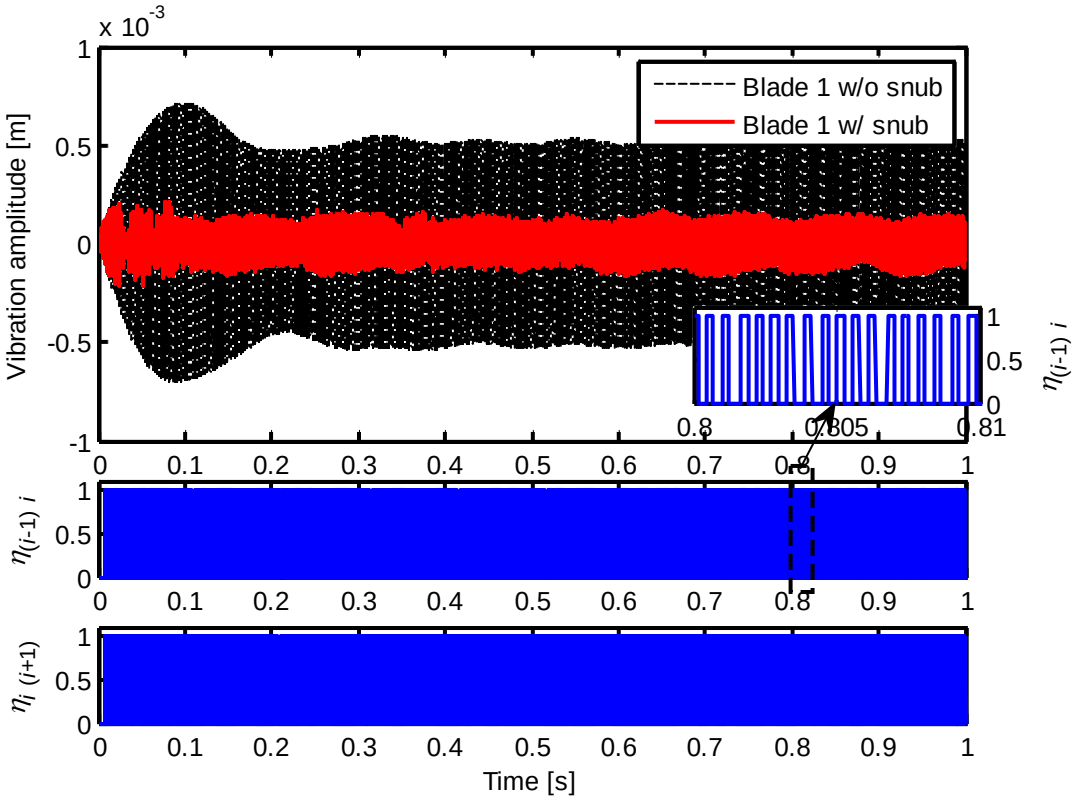

Figure 13: Time response of blade 1, n = 4, ΔF_4 = 150 N, f_0 = 50 Hz with turbulence.

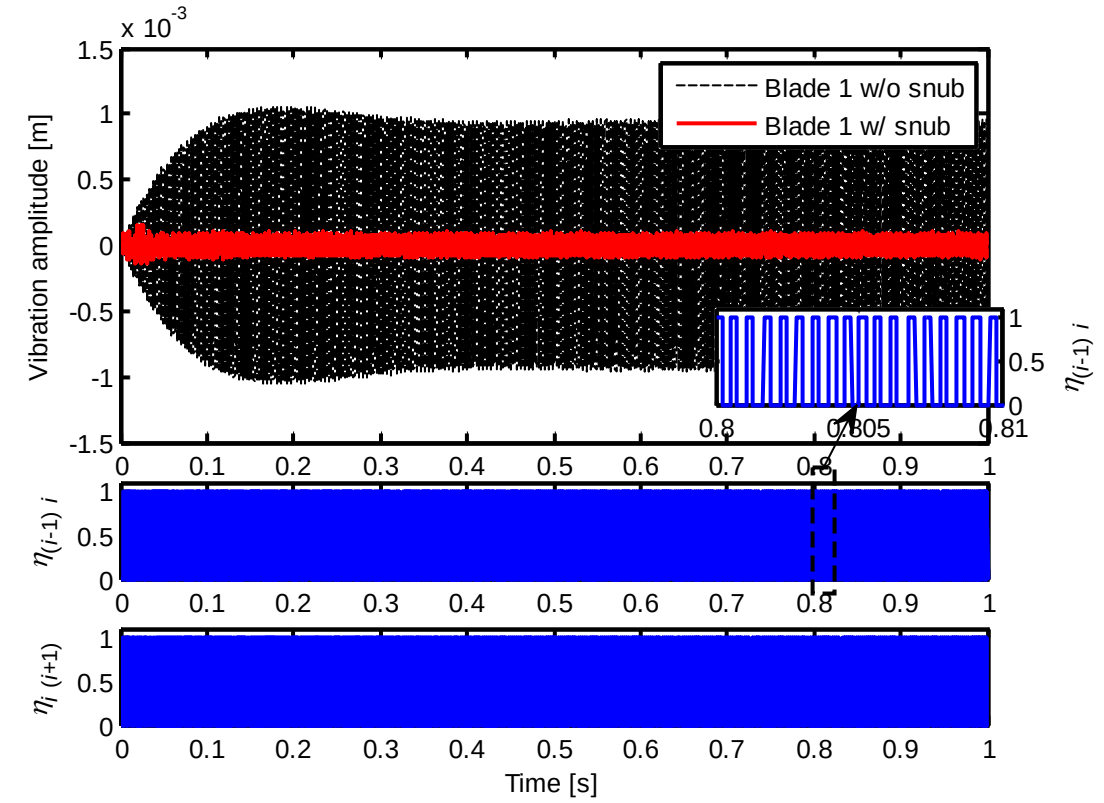

Figure 14: Time response of blade 1, n = 6, ΔF_6 = 150 N, f_0 = 50 Hz with turbulence.

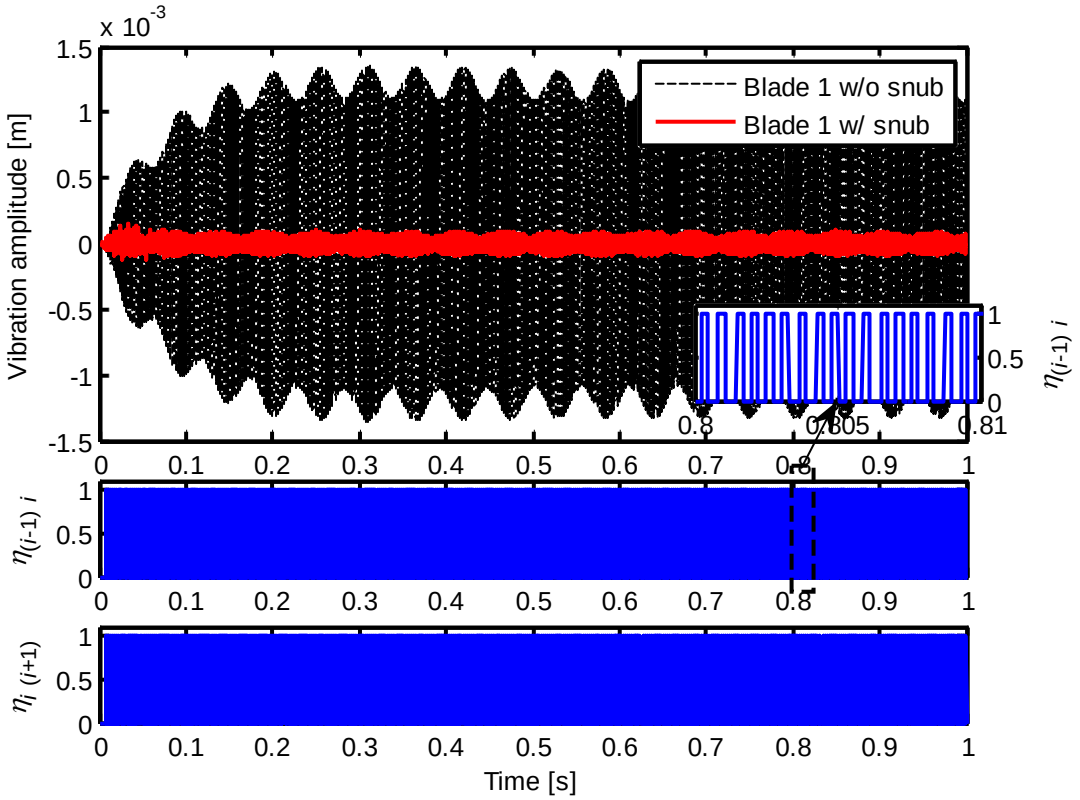

Figure 15: Time response of blade 1, n = 8, ΔF_8 = 150 N, f_0 = 50 Hz with turbulence.

Also the analysis of the steady-state vibration spectra of the three orders n considered is interesting and highlights relevant nonlinear behaviour. For the sake of brevity, only the spectrum corresponding to $n = 6$ is shown in figure 16. Apart from the exciting frequency corresponding to the blade frequency $f_b = nf_0 + f_t$, similarly to the previous case without turbulence, also the

eigenfrequency f_s of the bladed disk with integral shrouding is strongly excited. Anyhow, also the excitation at the frequency $|f_t - nf_0|$ appears as well as several sidebands of f_s, spaced of $\pm|f_t - nf_0|$, $\pm f_b$ and $\pm(f_b + |f_t - nf_0|)$. This complex structure of sidebands in the spectrum is present also for $n = 4$ and $n = 8$ and for all the blades of the row.

A counter-example, in which the snubbing is not effective in the reduction of the vibration with respect to free blades is shown in figure 17, that considers the time response, starting from initial null conditions, with the same external excitation on the row having the amplitude of 150 N, the rotating frequency $f_0 = 50\,\text{Hz}$ but only 2 nodal diameters. The excitation frequency is also in this case $f_b = 390.9\,\text{Hz}$, which is not close to eigenfrequency of 374.2 Hz associated to 2 nodal diameters, thus the system is not close to the resonant condition. The RMS value of the vibration amplitude is $x_{1,s}^{\text{RMS}} = 214.8\mu\text{m}$ in case of snubbing vs. $x_1^{\text{RMS}} = 108.9\mu\text{m}$ in case of free blades. Anyhow, in this case the blade with snubbing vibrates only about twice the corresponding free blade, whilst in the previous cases, when snubbing is effective, the reduction is of about an order of magnitude (see table 1).

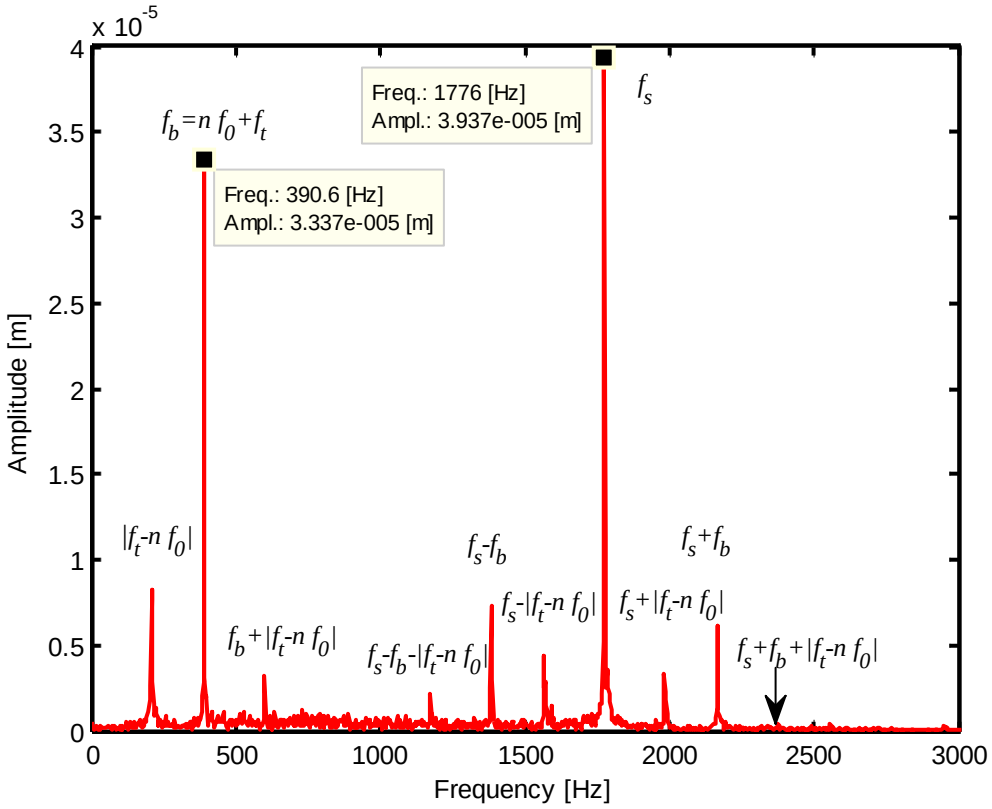

Figure 16: Vibration spectrum of blade 1 with snubbing, n = 6, ΔF_6 = 150 N, f_0 = 50 Hz with turbulence.

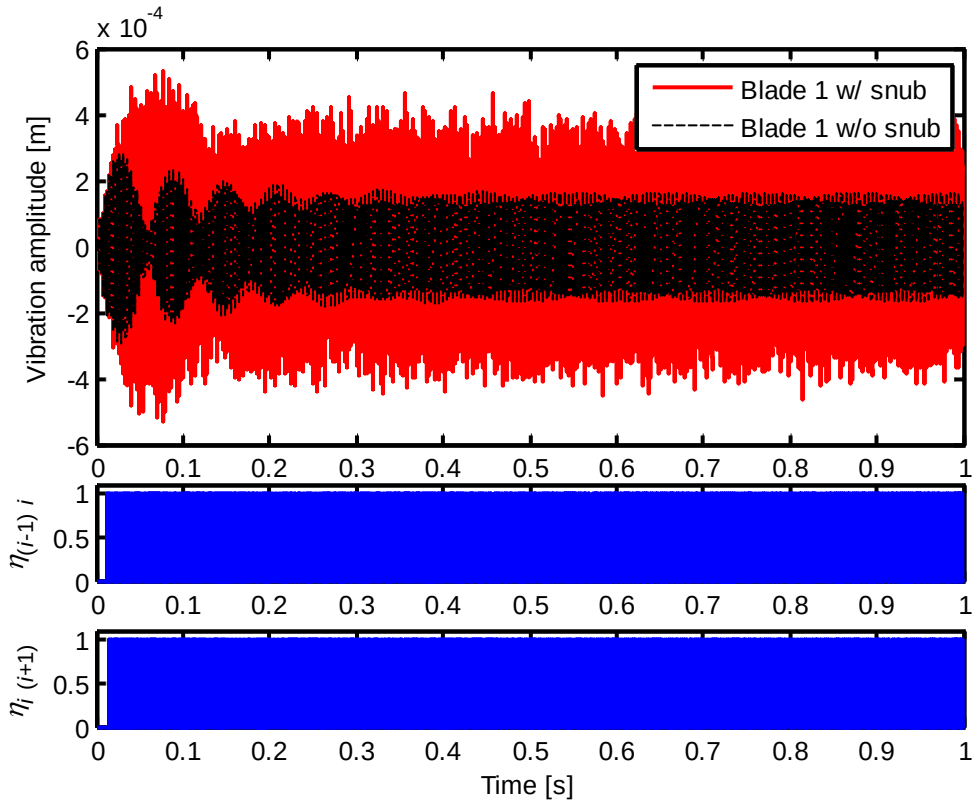

Figure 17: Time response of blade 1, $n = 2$, $\Delta F_2 = 150$ N, $f_0 = 50$ Hz.

7. CONCLUSIONS

The snubbing effect in bladed disks has been analyzed in this paper. A simple modal model is presented to analyze the dynamics of the snubbing over the entire row, with different exciting conditions. A suitable test-rig has been used to identify the modal parameters of an actual blade of a steam turbine. These values have then been used to simulate the effect of the snubbing on the entire row and to explore its actual effectiveness in blade vibration reduction. The examples show that, with the considered values of the excitation characteristics, not always snubbing reduces the blade vibration. Snubbing is effective when the bladed disk is excited in resonance or close to resonance, i.e. when the excitation frequency corresponds or is close to the eigenfrequency of a certain mode with a given number of nodal diameters. In these cases, the reduction of the vibration amplitude with respect to a free bladed disk is of an order of magnitude. If the excitation frequency is simply equal to the blade natural frequency and the number of nodal diameters is small, the bladed disk vibration can be higher if snubbing is present than in case of no contact between the shrouds, but the amplitude of the vibration is still of the same order of magnitude.

8. REFERENCES

[1] Mukhopadhyay N.K., Ghosh Chowdhury S., Das G., Chattoraj I., Das S.K. and Bhattacharya D.K., 1998, "An Investigation of the Failure of Low Pressure Steam Turbine Blades", *Engineering Failure Analysis*, **5**(3), doi:10.1016/S1350-6307(98)00016-8, pp. 181-193.

[2] Mazur Z., Hernández-Rossette A. and García-Illescas R., 2006, "Investigation of the Failure of the L-0 Blades", *Engineering Failure Analysis*, **13**(8), doi:10.1016/j.engfailanal.2005.10.018, pp. 1338-1350.

[3] Kubiak Sz. J., Urquiza B. G., García C. J. and Sierra E. F., 2007, "Failure Analysis of Steam Turbine Last Stage Blade Tenon and Shroud", *Engineering Failure Analysis*, 14(8), doi:10.1016/j.engfailanal.2007.01.012, pp. 1476-1487.

[4] Bréard C., Green J.S., Vahdati M. and Imregun M., 2001, "A Non-linear Integrated Aeroelasticity Method for the Prediction of Turbine Forced Response with Friction Dampers", *International Journal of Mechanical Sciences*, **43**, pp. 2715-2736.

[5] Sanliturk K.Y., Ewins D.J. and Stanbridge A.B., 2001, "Underplatform Dampers for Turbine Blades: Theoretical Modeling, Analysis, and Comparison With Experimental Data", *Journal of Engineering for Gas Turbines and Power*, **123**(4), doi: 10.1115/1.1385830, pp. 919-929.

[6] Berruti, T., Firrone, C.M., Pizzolante, M., Gola, M.M., 2007, "Fatigue damage prevention on turbine blades: Study of underplatform damper shape", *Key Engineering Materials*, **347**, pp. 159-164.

[7] Panning, L., Sextro, W., Popp, K., 2002 "Optimization of the contact geometry between turbine blades and underplatform dampers with respect to friction damping", *American Society of Mechanical Engineers, International Gas Turbine Institute, Turbo Expo (Publication) IGTI*, **4** B, pp. 991-1002.

[8] Panning, L., Popp, K., Sextro, W., Götting, F., Kayser, A., Wolter, I., 2004, "Asymmetrical underplatform dampers in gas turbine bladings: Theory and application", *Proceedings of the ASME Turbo Expo 2004*, **6**, pp. 269-280.

[9] Zucca, S., Botto, D., Gola, M.M., 2008, "Range of variability in the dynamics of semi-cylindrical friction dampers for turbine blades", Proceedings of the ASME Turbo Expo, **5**, PART A, pp. 519-529.

[10] Laxalde, D., Thouverez, F., Lombard, J.-P., 2007, "Vibration control for integrally bladed disks using friction ring dampers" Proceedings of the ASME Turbo Expo, **5**, pp. 255-265.

[11] Laxalde, D., Gibert, C., Thouverez, F., 2008 "Experimental and numerical investigations of friction rings damping of blisks", Proceedings of the ASME Turbo Expo, **5**, PART A, pp. 469-479.

[12] Laxalde, D., Thouverez, F., Lombard, J.-P., 2010, "Forced response analysis of integrally bladed disks with friction ring dampers", *Journal of Vibration and Acoustics, Transactions of the ASME*, **132**(1), pp. 0110131-0110139.

[13] Zmitrowicz A., 1996, "A Note on Natural Vibrations of Turbine Blade Assemblies with Non-continuous Shroud Rings", *Journal of Sound and Vibration*, **192**(2), 521-533.

[14] Sanliturk K.Y. and Ewins D.J., 1996, "Modelling Two-dimensional Friction Contact and its Application Using Harmonic Balance Method", *Journal of Sound and Vibration*, **193**(2), pp. 511-523.

[15] Yang B.D., Chu M.L. and Menq C.H., 1998, "Stick–Slip–Separation Analysis and Non-linear Stiffness and Damping Characterization of Friction Contacts Having Variable Normal Load", *Journal of Sound and Vibration*, **210**(4), 461-481.

[16] Petrov, E.P. and Ewins D.J., 2004, "Generic Friction Models for Time-Domain Vibration Analysis of Bladed Disks", *Journal of Turbomachinery*, **126**(1), doi: 10.1115/1.1644557, pp. 184-192.

[17] Petrov E.P., 2004, "Method for Direct Parametric Analysis of Nonlinear Forced Response of Bladed Disks with Friction Contact Interfaces", *Journal of Turbomachinery*, **126**(4), doi: 10.1115/1.1776588, pp. 654-662.

[18] Petrov E.P. and Ewins D.J., 2005, "Method for Analysis of Nonlinear Multiharmonic Vibrations of Mistuned Bladed Disks With Scatter of Contact Interface Characteristics", *Journal of Turbomachinery*, **127**(1), doi: 10.1115/1.1812781, pp. 128-136.

[19] Götting, F., Sextro, W., Panning, L., Popp, K., 2004, "Systematic mistuning of bladed disk assemblies with friction contacts", *Proceedings of the ASME Turbo Expo 2004*, **6**, pp. 257-266.

[20] Sextro, W., Panning, L., Götting, F., Popp, K., 2002, "Fast calculation of the statistics of the forced response of mistuned bladed disk assemblies with friction contacts", *American Society of Mechanical Engineers, International Gas Turbine Institute, Turbo Expo (Publication) IGTI*, **4** B, pp. 981-989.

[21] McVeigh P.A., Harish G., Farris T.N. and Szolwinski M.P., 1999, “Modeling interfacial conditions in nominally flat contacts for application to fretting fatigue of turbine engine components”, *International Journal of Fatigue*, **21**(S1), pp. S157-S165.

[22] Murthy H., Harish G. and Farris T.N. (2004) “Efficient Modeling of Fretting of Blade/Disk Contacts Including Load History Effects”, *ASME Journal of Tribology*, 126(1), doi: 10.1115/1.1540125, pp. 56-64.

[23] Golden P.J. and Calcaterra J.R.., 2006, “A Fracture Mechanics Life Prediction Methodology Applied to Dovetail Fretting”, *Tribology International*, **39**(10), doi: 10.1016/j.triboint.2006.02.006, pp. 1172-1180.

[24] Petrov, E.P. and Ewins D.J., 2003, “Analytical Formulation of Friction Interface Elements for Analysis of Nonlinear Multi-Harmonic Vibrations of Bladed Disks”, *Journal of Turbomachinery*, **125**(2), doi: 10.1115/1.1539868, pp. 364-371.

[25] Kielb J.J. and Abhari R.S., 2003, “Experimental Study of Aerodynamic and Structural Damping in a Full-Scale Rotating Turbine”, *Journal of Engineering for Gas Turbines and Power*, **125**(1), doi: 10.1115/1.1496776, pp. 103-112.